External Patch Group Prior Guided Internal Prior Learning for Real Image Denoising

Anonymous CVPR submission

Paper ID ****

Abstract

For image denoising problem, the external and internal priors are playing key roles in many different methdos. External priors learn from external images to restore noisy images while internal ones exploit priors of given images for denoising. The external priors are more generative and efficient on recovering structures existing in most images while the internal priors are more adaptive on recovering detials existed in given noisy images. In this paper, we propose to employ the external patch group prior of images to guide the clustering of internal patch groups, and develop an external dictionary guided internal orthogonal dictionary learning algorithm for real image denoising. The internal orthogonal dictionary learning process has closed-form solutions and hence very efficient for online denoising. The experiments on standard datasets demonstrate that, that the proposed method achieves better performance than other state-of-the-art methods on real image denoising.

1. Introduction

Most vision systems, such as medical imaging and surveillance, need accurate feature extraction from high-quality images. The camera sensors and outdoor low light conditions will unavoidly bring noise to the captured images. The impact is that the image details will be lost or hardly visible. As a result, image denoising is an essential procedure for the reliability of these vision systems. In the research ara, image denoising is also an ideal platform for testing natural image models and provides high-quality images for other computer vision tasks such as image registration, segmentation, and pattern recognition, etc.

For several decades, there emerge numerous image denoising methods [1, 2, 3, 4, 5, 6, 7, 8, 9, 10, 11], and all of them focus mainly on dealing with additive white Gaussian noise (AWGN). In real world, the cameras will undertake high ISO settings for high-speed shots on actions, long exposure for low light on night shots, etc. Under these situations, the noise is generated in a complex form and also been changed during the in-camera imaging pipeline [12, 13]. Therefore, the noise in real images are much more complex than Gaussian [13, 14]. It depends on camera series, brands, as well as the settings (ISO, shutter speed, and aperture, etc). The models designed for AWGN would become much less effective on real noisy images.

In the last decade, the methods of [15, 16, 17, 18, 19, 20, 13] are developed to deal with real noisy images. Almost all these methods employ a two-stage framework: estimating the parameters of the assumed noise model (usually Gaussian) and performing denoising with the help of the noise modeling and estimation in the first stage. However, the Gaussian assumption is inflexible in describing the complex noise on real noisy images [17]. Although the mixture of Gaussians (MoG) model is possible to approximate any noise distribution [21], estimating its parameters is time consuming via nonparametric Bayesian techniques [20]. To evaluate the performanec of these methods on dealing with complex real noise, we apply these methods, with corresponding default parameters, on a real noisy image provided in [13]. The testing image is captured by a Nikon D800 camera when ISO is 3200. The "ground truth" image is also provided with which we can calculate objective measurements such as PSNR and SSIM [22]. The denoised images are listed in Figure 1, from which we can see that these methods either remove the noise or oversmooth the complex details in real noisy image.

The above mentioned methods can be categorized into external methods which learn priors from external images to recover noisy images, and internal ones which exploit priors of given images for denoising. The external priors in natural images are free of the high correlation between noise and siganls in real noisy images, while the internal prior is adaptive to the image and can recover better the latent clean image. Combining the priors of external clean images and adaptivety of internal testing images can naturally improve the performance of denoising methods, especially on real noisy images. Based on these observations, in this paper, we propose to employ the external patch group prior [10]

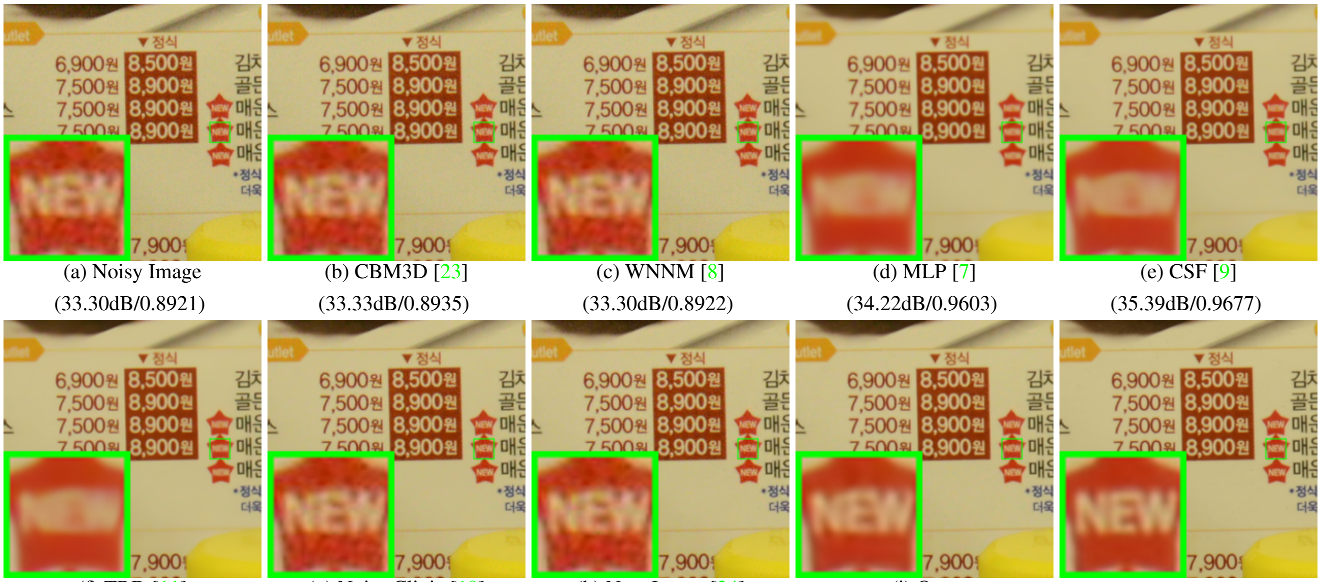

(a) Noisy Image (33.30dB/0.8921) (b) CBM3D [23] (33.33dB/0.8935) (c) WNNM [8] (33.30dB/0.8922) (d) MLP [7] (34.22dB/0.9603) (e) CSF [9] (35.39dB/0.9677)

(f) TRD [11] (35.97dB/0.9705) (g) Noise Clinic [19] (35.33dB/0.9520) (h) Neat Image [24] (34.39dB/0.9314) (i) Ours (**37.28**dB/**0.9729**) (j) Mean Image

Figure 1. Denoised images of the real noisy image "Nikon D800 ISO 3200 A3" from [13] by different methods. The images are better viewed by zooming in on screen.

of natural clean images to guide the clustering of internal patch groups in given noisy image, and develop an external prior guided internal orthogonal dictionary learning (DL) algorithm for real image denoising. The internal orthogonal DL process includes two alternating stages: updating sparse coefficients and updating orthogonal dictionary. Both of the two stages have closed-form solutions. Hence, our internal DL process is very efficient for online internal denoising. Through comprehensive experiments on real noisy images captured by different cameras and settings, we demonstrate that the proposed method achieves better performance on real image denoising

1.1. Our Contributions

The contributions of this paper are summarized as follows:

- We propose a novel model to learn internal priors adaptive to given images. This model employs the external patch group (PG) prior learned from clean images to guide the internal PG prior learning of given images. The external prior benefits the internal learning on subspace selection and orthogonal dictionary learning.
- The proposed guided internal prior learning method is very efficient. The reason is that both the subspace selection and orthogonal dictionary learning have explicit solutions.
- For real image denoising problem, the proposed method achieves much better performance than other competing methods.

The rest of this paper will be summerized as follows: in Section 2, we briefly introduce the related work; in Section 3, we develop the proposed external prior guided internal prior learning model; in Section 4, we formulate the overall image denoising algorithm; in Section 4, we demonstrate extensive experiments on real image denoising probelm; in Section 5, we conclude our paper and give future work.

2. Related Work

2.1. Patch Group Prior of Natural Images

The Patch Group (PG) prior [10] is proposed to directly model the non-local self similar (NSS) property of natural images. The NSS property is commonly used in image restoration tasks [1, 4, 5, 8, 10]. The PG prior largely reduces the space of images to be modeled when compared to the patch prior [6]. In [10], only the PGs of clean natural images is utilized, while the PGs of noisy input images are ignored. In this paper, we make use of PGs both from external clean images and internal given real noisy image for better denoising performance.

2.2. Internal v.s. External Prior Learning

Learning priors to represent images has been successfully used in image modeling [3, 6, 10, 25, 33]. There are mainly two categories of prior learning methods: 1) External methods pre-learned priors (e.g., dictionaries) from a set of clean images, and the learned priors are used to recover the noisy images [6, 10]. 2) Internal methods directly learned priors from the given noisy image, and the image denoising is simultaneously done with the learning process

[3, 25, 33]. Both the two categories of methods have limitations. The external methods is not adaptive to the noisy image, while the internal methods ignores the information hidden in clean images. In this paper, our goal is to employ the external prior to guide the internal prior learning.

2.3. Real Image Denoising

In the last decade, there are many methods [15, 16, 17, 18, 19, 20, 13] proposed for real image denoising problem. In the seminar work of BLS-GSM [30] for real image denoising, Portilla et al. proposed to use scale mixture of Gaussian in overcomplete oriented pyramids to estimate the latent clean images. In [15], Portilla proposed to use a correlated Gaussian model for noise estimation of each wavelet subband. The work of Rabie [16] modeled the noisy pixels as outliers which are removed via Lorentzian robust estimator [31]. Liu et al. [17] proposed to use 'noise level function' to estimate the noise and then use Gaussian conditional random field to obtain the latent clean image. Gong et al. [18] models the noise by mixed ℓ_1 and ℓ_2 norms and remove the noise by sparsity prior in the wavelet transform domain. Later, Lebrun el al. proposed a multiscale denoising algorithm called 'Noise Clinic' [19]. This method generalizes the NL-Bayes model [32] to deal with blind noise and achieves state-of-the-art performance. Recently, Zhu et al. proposed a Bayesian model [20] which approximates and removes the noise via Low-Rank Mixture of Gaussians.

3. External Patch Group Prior Guided Internal Prior Learning

In this section, we formulate the framework of external patch group (PG) prior guided internal orthogonal dictionary learning. We first introduce the patch PG leaning on clean natural RGB images. Then we propose to exploy the external PG prior to guide the internal clustering and orthogonal dictionary learning (DL). The orthogonal DL has alternative closed-form solutions in term of updating sparse coefficients and dictionary. Finally, we discuss the advantages of our proposed external PG prior guided internal orthogonal dictionary learning algorithm.

3.1. External Patch Group Prior Learning

Natural images often demonstrate repepitive local patterns, this nonlocal self-similarity (NSS) property is a key successful factor for many image denoising methods [1, 4, 5, 33, 8, 10]. In this section, we formulate the Patch Group prior learned on natural color images. Similar to [10], the patch group (PG) is defined as a group of similar patches to the local patch. The patch group mean is destracted, and hence different groups patches can share similar PGs. In this way, the space natural image patches to be modeled is largely reduced.

In this work, each local patch extracted from RGB images is of size $p \times p \times 3$. Then we search the M most similar patches $\{\mathbf{x}_m\}_{m=1}^{M}$ around each local patch through Euclidean distance, in a local window of size $W \times W$. The $\mathbf{x}_m \in \mathbb{R}^{3p^2 \times 1}$ is a patch vector formed by combining the 3 patch vectors (of size $p^2 \times 1$) in R, G, B channels. The mean vector of this PG is $\boldsymbol{\mu} = \frac{1}{M}\sum_{m=1}^{M}\mathbf{x}_m$, and the group mean subtracted PG is defined as $\overline{\mathbf{X}} \triangleq \{\overline{\mathbf{x}}_m = \mathbf{x}_m - \boldsymbol{\mu}\}, m = 1, ..., M$. Assume we have extracted N PGs from a set of external natural images, and the n-th PG is defined as $\overline{\mathbf{X}}_n \triangleq \{\overline{\mathbf{x}}_{n,m}\}_{m=1}^{M}, n = 1, ..., N$. We employ the Gaussian Mixture Model (GMM) to learn the external patch group based NSS prior. In this model, the likelihood of the n-th PG $\{\overline{\mathbf{X}}_n\}$ can be calculated as

$$P(\overline{\mathbf{X}}_n) = \sum_{k=1}^{K}\pi_k \prod_{m=1}^{M}\mathcal{N}(\overline{\mathbf{x}}_{n,m}|\boldsymbol{\mu}_k, \boldsymbol{\Sigma}_k), \quad (1)$$

where K is the number of Gaussians and the parameters π_k, $\boldsymbol{\mu}_k$, $\boldsymbol{\Sigma}_k$ are mixture weight, mean vector, and covariance matrix of the k-th Gaussian, respectively. By assuming that all the PGs are independently sampled, the overall objective log-likelihood function is

$$\ln \mathcal{L} = \sum_{n=1}^{N}\ln(\sum_{k=1}^{K}\pi_k \prod_{m=1}^{M}\mathcal{N}(\overline{\mathbf{x}}_{n,m}|\boldsymbol{\mu}_k, \boldsymbol{\Sigma}_k)). \quad (2)$$

We maximize the above objective function via EM algorithm [35] and finally obtain the GMM model with learned parameters. Similar to [10], the mean vector of each cluster is natural zeros, i.e., $\boldsymbol{\mu}_k = \mathbf{0}$.

Now, we have clustered the PGs extracted from external clean images into K Gaussians or subspaces. For notation simplicity, we ignore the index of subspace k. To better characterize each subspace, we perform singular value decomposition (SVD) on the covariance matrix:

$$\boldsymbol{\Sigma} = \mathbf{U}_e\mathbf{S}_e\mathbf{V}_e^T. \quad (3)$$

The singular vectors in $\mathbf{U}_e$ are employed as the external orthogonal dictionary to guide the internal orthogonal dictionary learning (the singular values are employed as prior weights for sparse coding which will be discussed in Section 4). For a dictionary $\mathbf{D}$, its *mutual incoherence* $\mu(\mathbf{D})$ [36] difined by

$$\mu(\mathbf{D}) = \max_{i=j}\frac{|\mathbf{d}_i^T\mathbf{d}_j|}{\|\mathbf{d}_i\|_2\|\mathbf{d}_j\|_2} \quad (4)$$

is a measure of quality of dictionary (lower is better). The dictionary $\mathbf{U}_e$ always has 0 *mutual incoherence* and hence better quality than non-orthogonal dictionaries.

3.2. External Prior Guided Internal Prior Learning

After the external patch group (PG) prior is learned, we can employ it to guide the internal PG prior learning for the given testing (real noisy) image. The guidance mainly comes from two aspects. One aspect is that the external prior can guide the internal noisy PGs to be assigned to most suitable Gaussians or subspaces. And for each subspace, the other aspect is to guide the orthogonal dictionary learning of internal noisy PGs.

3.2.1 Guided Internal Subspace Selection

Given a real noisy image, we extract the noisy PGs and corresponding mean vectors. Each mean substracted PG is defined as $\overline{\mathbf{Y}} \triangleq \{\overline{\mathbf{x}}_m\}_{m=1}^{M}$. Noted that, different from the external PGs, the mean vectors of the internal noisy PGs are saved for recovering. For adaptivity, we project the PG $\overline{\mathbf{Y}}$ into its most suitable Gaussian component (subspace) of the GMM learned on external PGs. The subspace most suitable for $\overline{\mathbf{Y}}$ is selected by firstly calculating the posterior probability of "$\overline{\mathbf{Y}}$ belonging to the kth Gaussian component":

$$P(k|\overline{\mathbf{Y}}) = \frac{\prod_{m=1}^{M} \mathcal{N}(\overline{\mathbf{y}}_m|\mathbf{0}, \mathbf{\Sigma}_k)}{\sum_{l=1}^{K} \prod_{m=1}^{M} \mathcal{N}(\overline{\mathbf{y}}_m|\mathbf{0}, \mathbf{\Sigma}_l)}, \tag{5}$$

and then choosing the component with the maximum A-posteriori (MAP) probability $\ln P(k|\overline{\mathbf{Y}})$.

3.2.2 Guided Internal Orthogonal Dictionary Learning

Now we have assigned all internal noisy PGs to their corresponding most suitable Gaussians or subspaces in $\{\mathcal{N}(\mathbf{0}, \mathbf{\Sigma}_k)\}_{k=1}^{K}$. For each subspace, we consider to use the external orthogonal dictionary to guide the learning of an orthogonal dictionary $\mathbf{D} := [\mathbf{D}_e\ \mathbf{D}_i] \in \mathbb{R}^{3p^2 \times 3p^2}$. This dictionary has two parts: the external part $\mathbf{D}_e \in \mathbb{R}^{3p^2 \times (3p^2 - r)}$ is consisted of the first $(3p^2 - r)$ columns of the singular vector matrix $\mathbf{U}_e$ obtained from the external prior by Equ. (3), and the internal part $\mathbf{D}_i$ is consisted of adaptive dictionary atoms learned from the internal noisy PGs. The learning is performed under the sparse coding framework (along with which the denoising of real noisy image is simultaneously done) as follows:

$$\begin{aligned} &\min_{\mathbf{D}_i \in \mathbb{R}^{3p^2 \times r}, \mathbf{A} \in \mathbb{R}^{3p^2 \times MN}} \|\mathbf{Y} - [\mathbf{D}_e\ \mathbf{D}_i]\mathbf{A}\|_F^2 + \lambda \|\mathbf{A}\|_1 \\ &\text{s.t.} \quad \mathbf{D}_i^T \mathbf{D}_i = \mathbf{I}_r,\ \mathbf{D}_e^T \mathbf{D}_i = \mathbf{0}, \end{aligned} \tag{6}$$

Similar to the K-SVD [3], we employ an alternating iterative framework to solve the optimization problem 4. In fact, we initialize the orthogonal dictionary as $\mathbf{D}^{(0)}$ and for $t = 0, 1, ..., T-1$, alternatively do:

Updating Sparse Coefficients: given the orthogonal dictioanry $\mathbf{D}_i^{(t)}$, we update the sparce coefficients via solving

$$\mathbf{A}^{(t)} := \arg\min_{\mathbf{A} \in \mathbb{R}^{3p^2 \times MN}} \|\mathbf{Y} - [\mathbf{D}_e\ \mathbf{D}_i^{(t)}]\mathbf{A}\|_F^2 + \lambda \|\mathbf{A}\|_1. \tag{7}$$

This problem has closed-form solution by $\mathbf{A}^* = T_\lambda(\hat{\mathbf{D}}^T \mathbf{Y})$, where $T_\lambda(\mathbf{A}) = \text{sgn}(\mathbf{A}) \odot \max(\mathbf{A}, \lambda)$ is a soft-thresholding function.

Updating Orthogonal Dictionary: given the sparse coefficients $\mathbf{A}^{(t)}$, we update the orthogonal dictionary via solving

$$\begin{aligned} \mathbf{D}_i^{(t+1)} := &\arg\min_{\mathbf{D}_i \in \mathbb{R}^{3p^2 \times r}} \|\mathbf{Y} - [\mathbf{D}_e\ \mathbf{D}_i]\mathbf{A}^{(t)}\|_F^2 \\ &\text{s.t.} \quad \mathbf{D}_i^T \mathbf{D}_i = \mathbf{I}_r,\ \mathbf{D}_e^T \mathbf{D}_i = \mathbf{0}, \end{aligned} \tag{8}$$

The sparse coefficients $\mathbf{A} = [\mathbf{A}_e^T\ \mathbf{A}_i^T]^T$ also has two parts: the external part $\mathbf{A}_e$ and the internal part $\mathbf{A}_i$ denote the coefficients over external dictionary $\mathbf{D}_e$ and internal dictionary $\mathbf{D}_i$, respectively. According to the Proposition 2.2 in [34], the problem (6) has a closed-form solution $\mathbf{D}_i^* = \mathbf{U}\mathbf{V}^T$, where $\mathbf{U}$ and $\mathbf{V}$ are the orthogonal matrices obtained by the following SVD

$$(\mathbf{I} - \mathbf{D}_e \mathbf{D}_e^T)\mathbf{Y}\mathbf{A}_i^T = \mathbf{U}\Sigma\mathbf{V}^T \tag{9}$$

With these solutions, the final obtained dictionary $\mathbf{D} = [\mathbf{D}_e\ \mathbf{D}_i]$ are orthogonal ictionary. This can be proved by the following equation

$$\mathbf{D}^T\mathbf{D} = \begin{bmatrix} \mathbf{D}_e^T \\ \mathbf{D}_i^T \end{bmatrix} [\mathbf{D}_e\ \mathbf{D}_i] = \begin{bmatrix} \mathbf{D}_e^T\mathbf{D}_e & \mathbf{D}_e^T\mathbf{D}_i \\ \mathbf{D}_i^T\mathbf{D}_e & \mathbf{D}_i^T\mathbf{D}_i \end{bmatrix} = \mathbf{I} \tag{10}$$

3.3. Discussions

Until now, we have divided the noisy PGs into multiple internal subspaces. Here we take a deep analysis on how the external NSS prior guide the subspace learning of internal PGs. The help are at least threefold. Firstly, through MAP in (3), the external prior guides the noisy PGs to be clustered into the correct subspaces. If we cluster the noisy PGs in an automatical way, the subspaces we learned will be highly degraded by the signal dependent noise. Secondly, the guidance of external prior for internal clustering is more efficient than directly clustering the internal noisy PGs. It only needs to calculate the MAP probability via the equation (3) while the internal clustering via GMM is time-consuming on EM algorithm [35]. Thirdly, due to the correct guidance of external prior, the structual decomposition via SVD of each subspace is more adaptive. This will bring better denoising performance than the methods only using the external information.

Through SVD, the PGs in each internal subspace can be divided into singular vectors and singular values. The singular vectors are the basis of the corresponding subspace while the singular values reflect the importance of these basis. The basis can be used as dictionary to code the noisy PGs. And the sigular values are adaptive parameters for internal noisy PGs. We can compare the singular values of one internal subspace and the corresponding space of external PGs. The result is shown in Figure **??**. From which we can see that the noisy subspace often have higher values than external space consisted of clean PGs. This gap is clearly made of the noise and can be used for image denoising in a natural way.

4. The Denoising Algorithm

4.1. Fast Patch Group Searching by Integral Image

The searching of patch groups in images is inefficient if we search non-local similar patches to each local patch. To speed up the searching process and make our proposed method faster, we employ the technique of 'Summed Area Table' [37] for efficient PG searching. The SAT permits to evaluate the sum of pixel values in rectangular regions of the image with four operations, regardless of the region size. That is to say, we do not need do distance measure for each patch. It was first proposed under the name of summed area table[38]

4.2. Prior Weights for Sparse Coding

To remove the real noise, we employ the sparse coding framework. And in order to be adaptive to the input image, we employ the internal learned $\mathbf{U}$ of each cluster as an adaptive dictioanry to represent the structural variations of the PGs in that cluster. Since the $\mathbf{U}$ is orthonormal, its *mutual incoherence* is naturally 0 and therefore better than other redundant dictionaries.

$$\min_{\boldsymbol{\alpha}} \|\overline{\mathbf{y}}_m - \mathbf{U}\boldsymbol{\alpha}\|_2^2 + \sum_{i=1}^{3p^2} \lambda_i |\boldsymbol{\alpha}_i|. \tag{11}$$

The ith entry of the regularization parameter λ_i

$$\lambda_i = \lambda/(\mathbf{S}_i + \varepsilon), \tag{12}$$

where ε is a small positive number to avoid dividing by zero. Since the dictionary $\mathbf{U}$ is orthonormal, it is not difficult to find out that (4) has a closed-form solution (detailed derivation can be found in the supplementary material):

$$\hat{\boldsymbol{\alpha}} = \text{sgn}(\mathbf{U}^{\mathbf{T}}\overline{\mathbf{y}}_m) \odot \max(|\mathbf{U}^{\mathbf{T}}\overline{\mathbf{y}}_m| - \boldsymbol{\Lambda}, \mathbf{0}), \tag{13}$$

where $\boldsymbol{\Lambda} = [\lambda_1, \lambda_2, ..., \lambda_{3p^2}]$ is the vector of regularization parameter and $\text{sgn}(\bullet)$ is the sign function, $\odot$ means element-wise multiplication, and $|\mathbf{U}^{\mathbf{T}}\overline{\mathbf{y}}_m|$ is the absolute value of each entry of vector $|\mathbf{U}^{\mathbf{T}}\overline{\mathbf{y}}_m|$. The closed-form solution makes our weighted sparse coding process very efficient.

4.3. The Overall Algorithm

With the solution $\hat{\boldsymbol{\alpha}}$ in (7), the clean patch in a PG can be estimated as $\hat{\mathbf{x}}_m = \mathbf{D}\hat{\boldsymbol{\alpha}} + \boldsymbol{\mu}_y$. Then the clean image $\hat{\mathbf{x}}$ can be reconstructed by aggregating all the estimated PGs. In practice, we could perform the above denoising procedures for several iterations for better denoising outputs. In iteration t, we use the iterative regularization strategy [39] to add back to the recovered image $\hat{\mathbf{x}}^{(t-1)}$ some estimation residual in iteration $t-1$. The proposed denoising algorithm is summarized in Algorithm 1 (Alg. 1).

Alg. 1: External Prior Guided Internal Orthogonal Dictionary Learning for Denoising

Input: Noisy image $\mathbf{y}$, PG-GMM model
1. Initialization: $\hat{\mathbf{x}}^{(0)} = \mathbf{y}, \mathbf{y}^{(0)} = \mathbf{y}$;
for $t = 1 : IteNum$ **do**
  for each PG $\mathbf{Y}$ **do**
2. Calculate group mean $\boldsymbol{\mu}_y$ and form PG $\overline{\mathbf{Y}}$;
3. Gaussian component selection via (3);
  end for
  for each Internal Subspace **do**
4. Internal Subspace Learning by (4);
5. Recover each patch in all PGs via $\hat{\mathbf{x}}_m = \mathbf{D}\hat{\boldsymbol{\alpha}} + \boldsymbol{\mu}_y$;
  end for
6. Aggregate the recovered PGs of all subspaces to form the recovered image $\hat{\mathbf{x}}^{(t)}$;
end for
Output: The recovered image $\hat{\mathbf{x}}^{(IteNum)}$.

Figure 2. Some testing images in the dataset [13].

Figure 3. Some cropped images of the dataset [13].

5. Experiments

In this section, we perform real image denoising experiments on three standard datasets. The first dataset is real noisy images with mean images as ground truths provided by [13], some samples are shown in Figure 3. The second dataset is provided by the website of Noise Clinic [19]. The third dataset is provided by the Commercial software Neat Image [24]. The second and third dataset do not have ground truth images.

5.1. Implementation Details

Our proposed method contains two stages, the external prior guided internal subspace learning stage and the adaptive denoising stage. In the learning stage, there are 4 parameters: the patch size p, the number of patches in a PG M, the window size W for PG searching and the number of

Table 1. Average PSNR(dB)/SSIM results of external, internal, and guided methods on 60 cropped real noisy images in [13].

	Noisy	Offline	Online	Guided
PSNR	34.51	38.19	38.07	**38.55**
SSIM	0.8718	0.9663	0.9625	**0.9675**

clusters K. We set $p = 6$ (hence the patch size is $6 \times 6 \times 3$), $M = 10$, $W = 31$, $K = 32$. We extracted about 3.6 million PGs from the Kodak PhotoCD Dataset, which includes 24 high quality color images, to train the external prior via PG-GMM. In the denoising stage, the paramter $\lambda = 0.002$ is used to regularize the sparse term. The δ in iterative regularization is set as $\delta = 0.09$.

5.2. Comparison on External and Internal methods

In this subsection, we compared the proposed external prior guided internal subspace learning model on real image denoising. The three methods are evaluated on the dataset provided in [13]. We calculate the PSNR, SSIM [22] and visual quality of these three methods. We also compare the speed. The PSNR and SSIM results on 60 cropped images from [13] are listed in Table 1. The images are cropped into size of 500×500 for better illustration. We also compare the three methods on visual quality in Figure 5.2. Compare the denoised images listed in Figure 5.2 and Figure 5.2, we can see that the Offline method is better at edges, smooth regions while the Online method is good at complex textures. The reason is two folds. Firstly, the Offline method is learned on clean images and hence is better at representing edges, structuals, and smooth area. The online method is influenced by the noise and hence some noise cannot be removed. Secondly, the Online method is better at recovering complex area sicne they could learn adaptive dictionaries for the specific area. The Offline method cannot recover the complex area since they did not learn the similar structures from the external natural clean images.

5.3. Comparison With other Competing Methods

We compare with previous state-of-the-art Gaussian noise removal methods such as BM3D [4], WNNM [8], MLP [7], CSF [9], and the recently proposed TRD [11]. We also compare with three competing real image denoising methods such as Noise Clinic, Neat Image, and the CC-Noise method proposed recently. The commercial software Neat Image [24] first estimates the parameters of noise via a large flat area and then filters the noise accordingly. All these methods need noise estimation which is vary hard to perform if there is no uniform regions are available in the testing image. The NeatImage will fail to perform automatical parameters settings if there is no uniform regions. [1]

We the competing denoising methods from various research directions on two datasets. Both the two datasets comes from the [13]. The first dataset contains 17 images of size over 7000×5000. Since this dataset contains repetitive contents across different images, we crop 60 small images of size 500×500 from these 17 images in [13]. The PSNR and SSIM resluts are listed in Table 3. The number in red color and blue color means the best and second best results, respectively. From the Table 3, we can see that the external based method can already surpass largely the previous denoising methods. The improvement on PSNR over the second best method, i.e., TRD, is 0.44dB. The

5.4. Discussion on Parameter λ

The proposed method only has a key parameter, namely the regularization paramters λ. To demonstrate that the proposed method is robust to the variance of λ, we vary the parameter λ across a wide range and obtain the PSNR and SSIM results as a function of the parameter λ. The results is shown in Figure 8, from which we can see that the proposed method can achieve a PSNR (SSIM) over 38.5dB (0.9660) when λ varies from 0.0015 to 0.0025. This shows that the proposed method is indeed robust to the chosen of the paramter λ.

6. Conclusion and Future Work

In the future, we will evaluate the proposed method on other computer vision tasks such as single image super-resolution, photo-sketch synthesis, and cross-domain image recognition. Our proposed method can be improved if we use better training images, fine tune the parameters via cross-validation. We believe that our framework can be useful not just for real image denoising, but for image super-resolution, image cross-style synthesis, and recognition tasks. This will be our line of future work.

References

[1] A. Buades, B. Coll, and J. M. Morel. A non-local algorithm for image denoising. *CVPR*, pages 60–65, 2005. 1, 2, 3

[2] S. Roth and M. J. Black. Fields of Experts. *International Journal of Computer Vision*, 82(2):205–229, 2009. 1

[3] M. Elad and M. Aharon. Image denoising via sparse and redundant representations over learned dictionaries. *Image Processing, IEEE Transactions on*, 15(12):3736–3745, 2006. 1, 2, 3, 4

[4] K. Dabov, A. Foi, V. Katkovnik, and K. Egiazarian. Image denoising by sparse 3-D transform-domain collaborative filtering. *Image Processing, IEEE Transactions on*, 16(8):2080–2095, 2007. 1, 2, 3, 6

[1] To compare with CCNoise, we first transform the denoised images into double format.

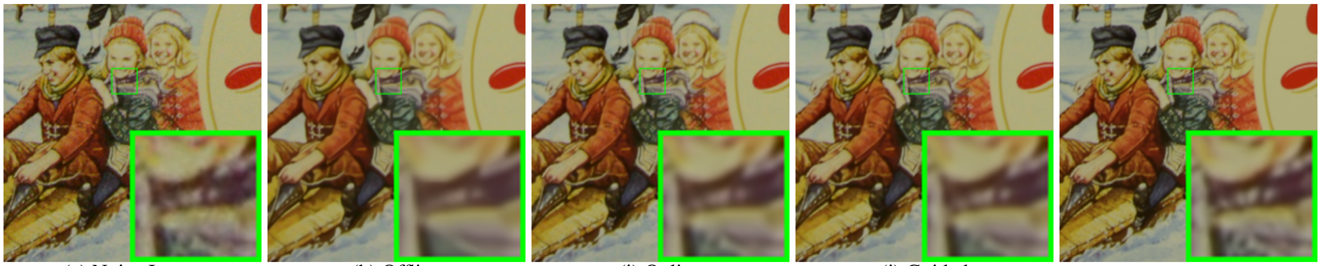

(a) Noisy Image (34.66dB/0.9178) | (h) Offline (34.97dB/0.9441) | (i) Online (36.86dB/0.9622) | (j) Guided (**37.09**dB/**0.9638**) | (h) Mean Image

Figure 4. Denoised images of the image "Nikon D600 ISO 3200 C1" by different methods. The images are better to be zoomed in on screen.

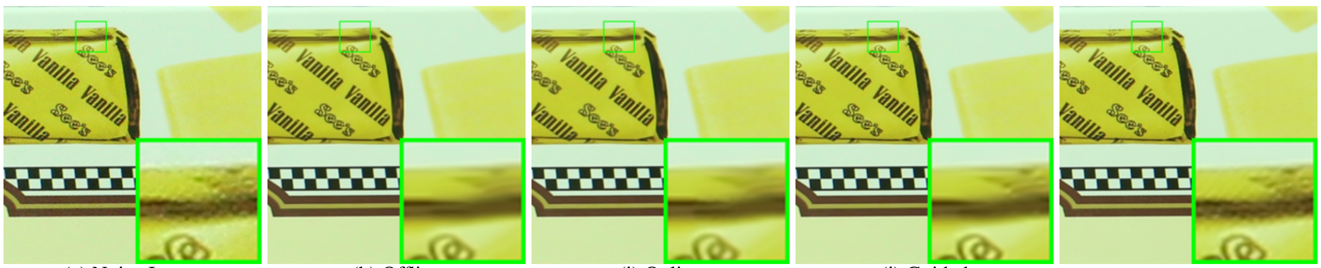

(a) Noisy Image (36.15dB/0.9523) | (h) Offline (37.12dB/0.9776) | (i) Online (35.70dB/0.9755) | (j) Guided (**37.94**dB/**0.9804**) | (h) Mean Image

Figure 5. Denoised images of the image "Canon EOS 5D Mark3 ISO 3200 C1" by different methods. The images are better to be zoomed in on screen.

[5] J. Mairal, F. Bach, J. Ponce, G. Sapiro, and A. Zisserman. Non-local sparse models for image restoration. *ICCV*, pages 2272–2279, 2009. 1, 2, 3

[6] D. Zoran and Y. Weiss. From learning models of natural image patches to whole image restoration. *ICCV*, pages 479–486, 2011. 1, 2

[7] Harold C Burger, Christian J Schuler, and Stefan Harmeling. Image denoising: Can plain neural networks compete with bm3d? *Computer Vision and Pattern Recognition (CVPR), 2012 IEEE Conference on*, pages 2392–2399, 2012. 1, 2, 6

[8] S. Gu, L. Zhang, W. Zuo, and X. Feng. Weighted nuclear norm minimization with application to image denoising. *CVPR*, pages 2862–2869, 2014. 1, 2, 3, 6

[9] U. Schmidt and S. Roth. Shrinkage fields for effective image restoration. *Computer Vision and Pattern Recognition (CVPR), 2014 IEEE Conference on*, pages 2774–2781, June 2014. 1, 2, 6

[10] J. Xu, L. Zhang, W. Zuo, D. Zhang, and X. Feng. Patch group based nonlocal self-similarity prior learning for image denoising. *2015 IEEE International Conference on Computer Vision (ICCV)*, pages 244–252, 2015. 1, 2, 3

[11] Yunjin Chen, Wei Yu, and Thomas Pock. On learning optimized reaction diffusion processes for effective image restoration. *Proceedings of the IEEE Conference on Computer Vision and Pattern Recognition*, pages 5261–5269, 2015. 1, 2, 6

[12] S. J. Kim, H. T. Lin, Z. Lu, S. Ssstrunk, S. Lin, and M. S. Brown. A new in-camera imaging model for color computer vision and its application. *IEEE Transactions on Pattern Analysis and Machine Intelligence*, 34(12):2289–2302, Dec 2012. 1

[13] Seonghyeon Nam, Youngbae Hwang, Yasuyuki Matsushita, and Seon Joo Kim. A holistic approach to cross-channel image noise modeling and its application to image denoising. *Proc. Computer Vision and Pattern Recognition (CVPR)*, pages 1683–1691, 2016. 1, 2, 3, 5, 6, 8

[14] Glenn E Healey and Raghava Kondepudy. Radiometric ccd camera calibration and noise estimation. *IEEE Transactions on Pattern Analysis and Machine Intelligence*, 16(3):267–276, 1994. 1

[15] J. Portilla. Full blind denoising through noise covariance estimation using gaussian scale mixtures in the wavelet domain. *Image Processing, 2004. ICIP '04. 2004 International Conference on*, 2:1217–1220, 2004. 1, 3

[16] Tamer Rabie. Robust estimation approach for blind denoising. *Image Processing, IEEE Transactions on*, 14(11):1755–1765, 2005. 1, 3

[17] C. Liu, R. Szeliski, S. Bing Kang, C. L. Zitnick, and W. T. Freeman. Automatic estimation and removal of noise from a single image. *IEEE Transactions on Pattern Analysis and Machine Intelligence*, 30(2):299–314, 2008. 1, 3

[18] Zheng Gong, Zuowei Shen, and Kim-Chuan Toh. Image restoration with mixed or unknown noises. *Multiscale Modeling & Simulation*, 12(2):458–487, 2014. 1, 3

Table 2. Average PSNR(dB) results of different methods on 60 cropped real noisy images captured in [13].

	Noisy	**CBM3D**	**WNNM**	**MLP**	**CSF**	**TRD**	**NI**	**NC**	**Guided**	**Guided2**
PSNR	34.51	34.58	34.52	36.19	37.40	37.75	36.53	37.57	38.72	38.90
SSIM	0.8718	0.8748	0.8743	0.9470	0.9598	0.9617	0.9241	0.9514	0.9694	0.9702

Table 3. Average PSNR(dB) results of different methods on 15 cropped real noisy images used in [13].

Camera Settings	**Noisy**	**CBM3D**	**WNNM**	**MLP**	**CSF**	**TRD**	**NI**	**NC**	**CC**	**Guided2**
Canon 5D Mark III ISO = 3200	37.00	37.08	37.09	33.92	35.68	36.20	37.68	38.76	38.37	40.50
	33.88	33.94	33.93	33.24	34.03	34.35	34.87	35.69	35.37	37.22
	33.83	33.88	33.90	32.37	32.63	33.10	34.77	35.54	34.91	37.13
Nikon D600 ISO = 3200	33.28	33.33	33.34	31.93	31.78	32.28	34.12	35.57	34.98	35.34
	33.77	33.85	33.79	34.15	35.16	35.34	35.36	36.70	35.95	36.69
	34.93	35.02	34.95	37.89	39.98	40.51	38.68	39.28	41.15	39.17
Nikon D800 ISO = 1600	35.47	35.54	35.57	33.77	34.84	35.09	37.34	38.01	37.99	38.82
	35.71	35.79	35.77	35.89	38.42	38.65	38.57	39.05	40.36	40.98
	34.81	34.92	34.95	34.25	35.79	35.85	37.87	38.20	38.30	38.90
Nikon D800 ISO = 3200	33.26	33.34	33.31	37.42	38.36	38.56	36.95	38.07	39.01	38.69
	32.89	32.95	32.96	34.88	35.53	35.76	35.09	35.72	36.75	36.82
	32.91	32.98	32.96	38.54	40.05	40.59	36.91	36.76	39.06	38.80
Nikon D800 ISO = 6400	29.63	29.66	29.71	33.59	34.08	34.25	31.28	33.49	34.61	33.31
	29.97	30.01	29.98	31.55	32.13	32.38	31.38	32.79	33.21	33.18
	29.87	29.90	29.95	31.42	31.52	31.76	31.40	32.86	33.22	33.35
Average PSNR	33.41	33.48	33.48	34.32	35.33	35.65	35.49	36.43	36.88	37.26
Average SSIM	0.8483	0.8511	0.8512	0.9113	0.9250	0.9280	0.9126	0.9364	0.9481	0.9505

[19] M. Lebrun, M. Colom, and J.-M. Morel. Multiscale image blind denoising. *Image Processing, IEEE Transactions on*, 24(10):3149–3161, 2015. 1, 2, 3, 5

[20] Fengyuan Zhu, Guangyong Chen, and Pheng-Ann Heng. From noise modeling to blind image denoising. *The IEEE Conference on Computer Vision and Pattern Recognition (CVPR)*, June 2016. 1, 3

[21] C. M. Bishop. *Pattern recognition and machine learning*. New York: Springer, 2006. 1

[22] Z. Wang, A. C. Bovik, H. R. Sheikh, and E. P. Simoncelli. Image quality assessment: from error visibility to structural similarity. *IEEE Transactions on Image Processing*, 13(4):600–612, 2004. 1, 6

[23] K. Dabov, A. Foi, V. Katkovnik, and K. Egiazarian. Color image denoising via sparse 3d collaborative filtering with grouping constraint in luminance-chrominance space. *IEEE International Conference on Image Processing*, 1, 2007. 2

[24] Neatlab ABSoft. Neat image. https://ni.neatvideo.com/home. 2, 5, 6

[25] G. Yu, G. Sapiro, and S. Mallat. Solving inverse problems with piecewise linear estimators: From Gaussian mixture models to structured sparsity. *IEEE Transactions on Image Processing*, 21(5):2481–2499, 2012. 2, 3

[26] Daniel Glasner, Shai Bagon, and Michal Irani. Super-resolution from a single image. *ICCV*, 2009.

[27] Maria Zontak, Inbar Mosseri, and Michal Irani. Separating signal from noise using patch recurrence across scales. *Proceedings of the IEEE Conference on Computer Vision and Pattern Recognition*, pages 1195–1202, 2013.

[28] Tomer Michaeli and Michal Irani. Blind deblurring using internal patch recurrence. *European Conference on Computer Vision*, pages 783–798, 2014.

[29] Y. Bahat and M. Irani. Blind dehazing using internal patch recurrence. *IEEE International Conference on Computational Photography (ICCP)*, pages 1–9, May 2016.

[30] J. Portilla, V. Strela, M.J. Wainwright, and E.P. Simoncelli. Image denoising using scale mixtures of Gaussians in the wavelet domain. *Image Processing, IEEE Transactions on*, 12(11):1338–1351, 2003. 3

[31] Peter J Huber. *Robust statistics*. Springer, 2011. 3

[32] M. Lebrun, A. Buades, and J. M. Morel. A nonlocal bayesian image denoising algorithm. *SIAM Journal on Imaging Sciences*, 6(3):1665–1688, 2013. 3

[33] W. Dong, L. Zhang, G. Shi, and X. Li. Nonlocally centralized sparse representation for image restoration. *Image Processing, IEEE Transactions on*, 22(4):1620–1630, 2013. 2, 3

[34] Chenglong Bao, Jian-Feng Cai, and Hui Ji. Fast sparsity-based orthogonal dictionary learning for image restoration. *Proceedings of the IEEE International Conference on Computer Vision*, pages 3384–3391, 2013. 4

(a) Noisy Image (37.00dB/0.9345) (b) CBM3D (37.02dB/0.9351) (c) WNNM (37.01dB/0.9347) (d) MLP (33.90dB/0.9171) (e) TRD (36.18dB/0.9454)

(f) Noise Clinic (38.76dB/0.9689) (g) Neat Image (37.68dB/0.9600) (h) CCNoise (38.37dB/0.9678) (i) Guided (**40.26**dB/**0.9800**) (j) Mean Image

Figure 6. Denoised images of the image "Canon 5D Mark 3 ISO 3200 1" by different methods. The images are better to be zoomed in on screen.

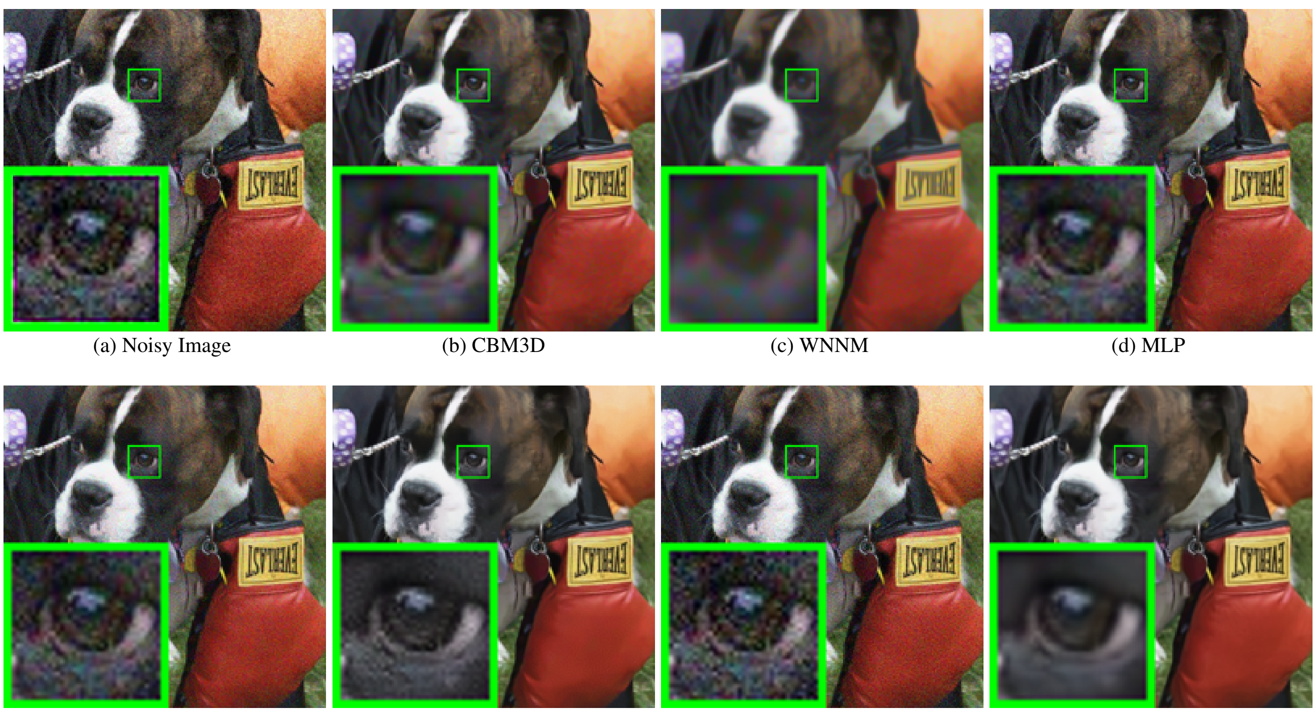

(a) Noisy Image (b) CBM3D (c) WNNM (d) MLP

(e) TRD (f) Noise Clinic (g) Neat Image (h) Guided

Figure 7. Denoised images of the image "$5dmark3iso32003$" by different methods. The images are better to be zoomed in on screen.

[35] A. P. Dempster, N. M. Laird, and D. B. Rubin. Maximum likelihood from incomplete data via the EM algorithm. *Journal of the Royal Statistical Society. Series B (methodological)*, pages 1–38, 1977. 3, 4

[36] David L Donoho and Michael Elad. Optimally sparse representation in general (nonorthogonal) dictionaries via 1 minimization. *Proceedings of the National Academy of Sciences*, 100(5):2197–2202, 2003. 3

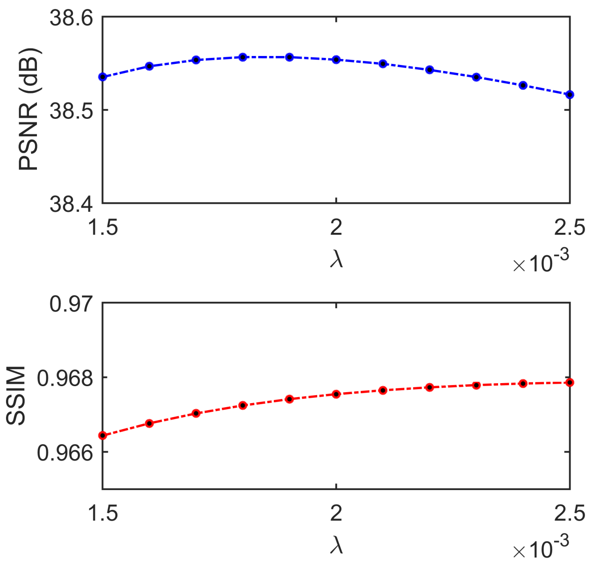

Figure 8. The PSNR/SSIM results as a function of the parameter λ.

[37] Franklin C. Crow. Summed-area tables for texture mapping. *SIGGRAPH Comput. Graph.*, 18(3):207–212, January 1984. 5

[38] Paul Viola and Michael J Jones. Robust real-time face detection. *International journal of computer vision*, 57(2):137–154, 2004. 5

[39] S. Osher, M. Burger, D. Goldfarb, J. Xu, and W. Yin. An iterative regularization method for total variation-based image restoration. *Multiscale Modeling & Simulation*, 4(2):460–489, 2005. 5